Semi-active Control of Seismically Excited Hysteretic Structures using Variable Viscous Dampers

Sami El-Borgi

Ecole Polytechnique de Tunisie, Tunisia

Fahim Sadek

National Institute of Standards and Technology, USA

Brahim Jemai

Faculté des Sciences de Gabes, Tunisia

Mohamed Amin Walha

Ecole Polytechnique de Tunisie, Tunisia

Michael Riley

National Institute of Standards and Technology USA

ABSTRACT

This paper describes the application of a semi-active variable viscous (SAVV) damper for reducing the response of a seismically excited hysteretic structure. Two algorithms for selecting the damping properties of the SAVV damper were used: the Linear Quadratic Regulator (LQR) and the Sliding Mode Control (SMC) algorithms. Both were formulated based on full-state feedback and static output feedback, with or without an observer. The equations of motion were formulated in the state-space and in the drift (inter-story) coordinate system. An eight-story shear building with a seismic isolation system supplemented with a SAVV was analyzed using the selected control algorithms and subjected to a strong earthquake. The results of the various analyses indicate that variable dampers can effectively reduce both the displacement and acceleration responses, and consequently, the story and base shears of both linear and hysteretic structures.

INTRODUCTION

Semi-active control devices combine the features of active and passive control to reduce the response of structures to various dynamic loadings. A significant amount of research and development has been conducted on these devices because of their relatively high performance and low energy requirement. Most research on semi-active control systems has been limited to linear structures (Symans and Constantinou [1995], Sadek and Mohraz [1998], Jansen and Dyke [1999]). Under strong earthquake excitations, however, structural members might experience yielding and the response will become non-linear. Few studies have

considered the performance of semi-active control for such hysteretic structures (El-Borgi, et al. [2000a,b]). The main purpose of this research is to examine the effectiveness of a semi-active variable viscous (SAVV) damper for reducing the hysteretic response of structures subjected to strong earthquakes.

SAVV dampers are designed such that their damping coefficient can be adjusted during a dynamic event. Several investigators have developed control algorithms for these devices, including a clipped optimal control algorithm (Sack [1994]), a bang-bang algorithm (Patten, et al. [1994]), a Linear Quadratic Regulator (LQR) algorithm (Symans and Constantinou [1995], Sadek and Mohraz [1998]), a Sliding Mode Control (SMC) algorithm (Symans and Constantinou [1995], Yang, et al. [1995]), a generalized LQR algorithm with a penalty on the acceleration response (Sadek and Mohraz [1998]), and a displacement-acceleration domain algorithm (Sadek and Mohraz [1998]).

In this paper, two algorithms for regulating the damping coefficient of the SAVV damper are described, Linear Quadratic Regulator (LQR) and the Sliding Mode Control (SMC). Both are formulated based on full-state feedback (FSF) and static output feedback (SOF) with or without an observer. The structures used in this study are modeled with a one-dimensional, shear-type building with a hysteretic behavior. The inelastic behavior is modeled using the Bouc-Wen hysteresis model. The variable viscous damper is simply modeled by a linear viscous element. Simulation results are obtained for an eight-story shear building with a seismic isolation system supplemented with a SAVV under the El Centro earthquake with a peak ground acceleration (PGA) of $0.3g$.

EQUATIONS OF MOTION OF CONTROLLED STRUCTURE

Consider an n-degree-of-freedom hysteretic structure equipped with m SAVV dampers and subjected to a one-dimensional earthquake ground excitation $\ddot{x}_g$. Its motion is described by:

$$M\ddot{x} + C\dot{x} + K_{el}x + K_{in}v = D\,u(t) + E\ddot{x}_g \tag{1}$$

where x is an n-dimension vector representing the relative inter-story displacement, u is an r-dimension vector representing the control forces generated by the SAVV dampers, M and C are the $n \times n$ element mass and damping matrices, D is the $n \times r$ element control force location matrix, E is an n-dimension mass vector representing the influence of the earthquake excitation, K_{el} and K_{in} are, respectively, the elastic and the inelastic stiffness matrices defined in Yang, et al. [1992], and v is the evolutionary hysteretic n-dimension vector representing the behavior of the structure where each of its components is modeled by the Bouc-Wen model (Wen [1976]) as follows:

$$\dot{v}_i = \left(D_{y_i}\right)^{-1}\left(A_i\dot{x}_i - \beta_i|\dot{x}_i||v_i|^{n_i-1} - \gamma_i\dot{x}_i|v_i|^{n_i}\right) \qquad i = 1,\cdots,n \tag{2}$$

Here, D_{y_i} is the yield deformation of the i-th story, and A_i, β_i, γ_i, and n_i define the scale, shape, and smoothness of the hysteresis loop corresponding to story i.

The state-space representation of Eq. (1) is given by:

$$\dot{z} = g(z) + Bu + H\ddot{x}_g \tag{3}$$

where $z = \{x \quad v \quad \dot{x}\}^T$ is the $3n$-dimension state vector, $g(z)$ is a $3n$-dimension vector, which is a nonlinear function of z, B is a $3n \times r$ element matrix, and H is a $3n$-dimension vector given by Yang, et al. [1992].

SEMI-ACTIVE CONTROL ALOGORITHMS

LQR Algorithm

This algorithm is the classical linear quadratic regulator, extensively used for active and semi-active control of structures. The control force, u, is obtained by minimizing the quadratic cost function, $J = \int_0^{t_f} \left(z^T Q z + u^T R u \right) dt$, over the duration of the excitation, t_f, when constrained by the linearized form of Eq. (3). Here, Q and R are positive semi-definite and positive definite weighting matrices, respectively. This results in the control force vector, $u = \left(-0.5 R^{-1} B^T P \right) z = G z$, where the matrix G represents the control gain and P is the solution of the classical Riccati equation.

For a SAVV damper modeled by a linear viscous damper, the maximum force is $\pm \widetilde{F}_{max}$, and the damping coefficient, $\widetilde{c}$, can be computed as: $\widetilde{c}_i = u_i / \dot{x}_i$, ($i$ = 1, ..., r) with $\widetilde{c}_i \in \left[\widetilde{c}_{min}, \widetilde{c}_{max} \right]$. Here, $\dot{x}_i$ is the relative velocity between the ends of the i-th damper, and $\widetilde{c}_{min}$ and $\widetilde{c}_{max}$ are the minimum and maximum damping coefficients.

SMC Algorithm

The SMC algorithm used in this study is similar to the one developed by Yang, et al. [1995] for active control. This algorithm is based on two steps: the first is the sliding surface design using an LQR algorithm, and the second is the controller design using the Lyapunov method. The design of the sliding surface, $S = \overline{P} Z = 0$, consists of obtaining the sliding matrix, $\overline{P}$, through the minimization of the performance index, $J = \int_0^{t_f} \left[z^T Q z \right] dt$, constrained by the linearized form of Eq. (3). In the expression of the cost function, Q is a positive semi-definite weighting matrix. The purpose of the controller design is to drive the response trajectory onto the sliding surface. The Lyapunov function $V = 0.5 S^T S$ is considered. The sufficient condition for the sliding mode to be stable is given by: $\dot{V} = S^T S \leq 0$. Using the state equation of motion, we obtain: $\dot{V} = \lambda^T \left(u - \overline{u} \right)$, where u is the control force, λ and $\overline{u}$ are expressed as $\lambda = S^T \overline{P} B$ and $\overline{u} = \left[\overline{P} B \right]^{-1} \overline{P} \left(A z + B'' v + H \ddot{x}_g \right)$. B'' is given by Yang, et al. [1992]. Using the control law, proposed by Yang, et al. [1995], $u = \overline{u} - \overline{\delta} \lambda^T$, in which $\overline{\delta}$ is called the sliding margin matrix and is user input, we obtain the expression for the control force regulated by both the structural response and the earthquake excitation: $u = G_1 z + G_2 \ddot{x}_g$. G_1 and G_2 are, respectively, the feedback and feedforward gain matrices. The same constraints imposed for the LQR algorithm are applied to the SMC algorithm.

Kalman-Bucy Filter

The linear Kalman-Bucy filter is used in the control loop to estimate the components of the state vector, z, from the measured output, y, of the following linearized form of Eq. (3):

$$\dot{z} = A z + B u + H \ddot{x}_g \qquad\qquad y = \overline{C} z + \overline{D} u + \overline{H} \ddot{x}_g + w \qquad\qquad (4a,b)$$

We assume the measurement noise, w, is a Gaussian process. The estimated state vector, $\hat{z}$, is given by the Kalman filter, $\dot{\hat{z}} = A\hat{z} + Bu + L\left(y - \overline{C}\hat{z} - \overline{D}u - H\ddot{x}_g\right)$, whose objective is to minimize the prediction error, $\varepsilon = \hat{z} - z$, in the least-square sense. L is the Kalman gain obtained as: $L = \left(PC^T + V\right)W^{-1}$, where V and W are, respectively, the covariance matrices of $H\ddot{x}_g$ and w, and P is the solution of Riccati equation: $PA + A^TP - PC^TW^{-1}CP + V = 0$. Therefore, in the control loop the estimated state vector is used to compute the necessary control action on the system using either the LQR or SMC algorithm. The control block diagram is illustrated in Figure 1.

NUMERICAL RESULTS

The eight-story seismic-isolated hysteretic structure used by Yang, et al. [1995] was considered in this work. The seismic isolation consists of rubber bearings supplemented with either an active control system or a SAVV damper. The structural parameters are summarized in Table 1. The maximum control force, and the maximum and minimum damping coefficients are, respectively, $\widetilde{F}_{\max} = 1000$ kN, $\widetilde{c}_{\max} = 41.4 \times 10^5$ kNs/m, and $\widetilde{c}_{\min} = 5.17 \times 10^5$ kNs/m. The structure was subjected to the El Centro earthquake with a PGA of 0.3g. The response was analyzed using the LQR and SMC algorithms for the active and semi-active control cases, with either full state feedback (FSF) or static output feedback (SOF). The Kalman-Bucy filter was used in conjunction with the SOF case. In this case, only the absolute accelerations at all story levels, including the seismic isolation, were measured for practical and economical reasons. For the case of the SMC algorithm with FSF or SOF, the ground acceleration was measured, as well. For the LQR algorithm, $R = 3.61 \times 10^{-11}$ and the matrix $Q = diag(5000, 5000, 5000, 5000, 5000, 5000, 5000, 5000, 0.01, 1, 1, 1, 1, 1, 1, 1, 1, 1)$. For the SMC algorithm, $\overline{\delta} = 5 \times 10^9$ and Q is the same as for the LQR algorithm.

The maximum response quantities are shown in Table 2 for the cases of: (1) no control; (2) passive seismic isolation; (3) active control using the LQR algorithm with FSF; (4) semi-active control using the LQR algorithm with FSF; (5) active control using the LQR algorithm with SOF; (6) semi-active control using the LQR algorithm with SOF; (7) active control using the SMC algorithm with FSF; (8) semi-active control using the SMC algorithm with FSF; (9) active control using the SMC algorithm with SOF; and (10) semi-active control using the SMC algorithm with SOF.

The results indicate the following: (a) the use of the isolation bearing dramatically reduces the response of the structure (linear super-structure) at the cost of large isolator displacements; (b) using active and semi-active control, the isolator displacement decreases substantially; (c) for active and semi-active control, the LQR algorithm results in smaller isolator displacement, but larger inter-story drifts and accelerations as compared with the SMC algorithm with the same force requirement; (d) semi-active control using SAVV dampers results in a response comparable to that using active control, considering that the larger semi-active displacements are accompanied by substantially reduced control forces; (e) for active and semi-active control using either LQR or SMC algorithms, the response with FSF, in terms of inter-story displacements or acceleration, is comparable to that with SOF with acceleration measurement.

CONCLUSION

The results of these simulations show the advantages of using both passive seismic isolation and isolation combined with active or semi-active control devices. The passive isolation produced the most significant performance improvement, but addition of the active and semi-active controllers further improved the structural response while reducing the drift in the isolation. Both the active and semi-active systems were able to reduce the displacements and drifts, without greatly increasing the accelerations. The sliding mode controllers tended to provide the best overall performance, minimizing both the drifts and story accelerations, without causing large displacements or accelerations in the isolation. Finally, one of the most important results was the performance of the system with the static output feedback. Even without measuring the full state vector, the controllers were able to produce responses that are nearly identical to the full state feedback controllers.

REFERENCES

El-Borgi, S., Riley, M., Sadek, F. and Ayed, N. (2000a) Semi-active Control of Linear and Hysteretic Structures using Variable Viscous and Magnetorheological Dampers, *Proceedings of the 2nd European Conference on Structural Control*, Paris, France.

El-Borgi, S. and Tsopelas, P. (2000b) Semi-active Control of 3-D Linear and Hysteretic Structures for Seismic Applications, *Proceedings of the 3rd International Workshop on Structural Control*, Paris, France.

Jansen, L.M. and Dyke, S.J. (1999) Semi-active Control Strategies for the MR Damper: A Comparative Study. *ASCE Journal of Engineering Mechanics*.

Patten, W.N., Kuo, C.C., He, Q., Liu, L. and Sack, R.L. (1994) Seismic Structural Control via Hydraulic Semi-active Vibration Dampers. *Proceedings of the 1st World Conference on Structural Control*, Los Angeles.

Sack, R.L., Kuo, C.C., Wu, H.C., Liu, L. and Patten, W.N. (1994) Seismic Motion Control via Semi-active Hydraulic Actuators. *Proceedings of the 5th U.S. National Earthquake Engineering Conference*.

Sadek, F. and Mohraz, B. (1998) Semi-active Control Algorithms for Structures with Variable Dampers. *ASCE Journal of Engineering Mechanics*.

Symans, M. D and Constantinou, M.C. (1995) Development and experimental study of semi-active fluid damping devices for seismic protection of structures. Report No. NCEER-95-0011, State Univ. of New York at Buffalo.

Yang, J.N., Li, Z. and Vongchavalitkul, S. (1992) A Generalization of Optimal Control Theory: Linear and Nonlinear Structures. Report No. NCEER-92-0026, State Univ. of New York at Buffalo.

Yang, J.N., Wu, J.C. and Agrawal, A.K. (1995) Sliding mode control for nonlinear and hysteretic structures. *ASCE Journal of Engineering Mechanics*.

Wen, Y.-K. (1976) Method for random vibration of hysteretic systems. *ASCE Journal of Engineering Mechanics*.

Table 1: Structural parameters of the eight-story building model

Story Number	Base	1	2	3	4	5	6	7	8
Mass (10^3 kg)	450	345.6	345.6	345.6	345.6	345.6	345.6	345.6	345.6
Damping (10^3 kNs/m)	26.17	490	467	410	386	349	298	243	196
Stiffness (10^3 kN/m)	18.05	340	320	285	269	243	207	169	137
Ratio of pre-yield to post-yield stiffness	0.6	0.1	0.1	0.1	0.1	0.1	0.1	0.1	0.1
Yield displacement (cm)	4.0	2.4	2.3	2.2	2.1	2.0	1.9	1.7	1.5

Table 2: Maximum response quantities of the building model under El Centro with PGA 0.3g
(D: Interstory-displacement (cm); A: Absolute acceleration (mm/sec^2))

	Story Number		Base	1	2	3	4	5	6	7	8
1	No Control	D	---	2.04	2.10	2.14	2.38	2.64	3.19	4.33	1.98
	U = 0 kN	A	---	380.4	433.4	494.8	458.9	561.2	463.7	590.4	614.9
2	Passive Isolation	D	21.37	0.62	0.60	0.65	0.63	0.63	0.64	0.60	0.41
	U = 0 kN	A	122.4	113.5	112.5	111.5	101.9	91.5	103.0	131.5	163.4
3	LQR-FSF-A	D	8.97	0.53	0.57	0.65	0.68	0.66	0.65	0.74	0.58
	U = 1270.0 kN	A	151.6	148.7	138.2	111.5	110.1	124.0	147.5	157.8	131.9
4	LQR-FSF-SA	D	9.15	0.52	0.54	0.61	0.65	0.65	0.65	0.74	0.58
	U = 1000.0 kN	A	151.6	148.7	137.9	135.9	114.4	114.8	140.5	157.7	231.9
5	LQR-SOF-A	D	8.95	0.53	0.57	0.66	0.68	0.66	0.65	0.75	0.59
	U = 1274.1 kN	A	152.1	149.2	138.5	111.9	110.4	124.3	148.1	158.2	232.7
6	LQR-SOF-SA	D	9.15	0.53	0.54	0.61	0.65	0.65	0.65	0.75	0.59
	U = 1000.0 kN	A	152.1	149.2	138.4	136.6	115.0	115.6	141.1	158.2	232.6
7	SMC-FSF-A	D	9.94	0.21	0.18	0.17	0.16	0.15	0.16	0.15	0.12
	U = 1270.0 kN	A	163.0	50.8	42.8	47.9	39.3	40.3	45.1	44.4	45.9
8	SMC-FSF-SA	D	12.65	0.22	0.20	0.19	0.18	0.18	0.17	0.16	0.12
	U = 1000.0 kN	A	240.5	47.7	34.9	39.5	38.8	43.8	45.0	46.0	46.4
9	SMC-SOF-A	D	9.82	0.21	0.18	0.17	0.16	0.15	0.16	0.15	0.12
	U = 1269.7 kN	A	163.6	50.7	43.0	48.1	39.3	40.1	45.3	44.7	46.0
10	SMC-SOF-SA	D	10.87	0.19	0.19	0.18	0.17	0.16	0.16	0.16	0.12
	U = 1000.0 kN	A	228.5	48.6	35.4	40.6	38.0	42.8	45.3	39.3	46.7
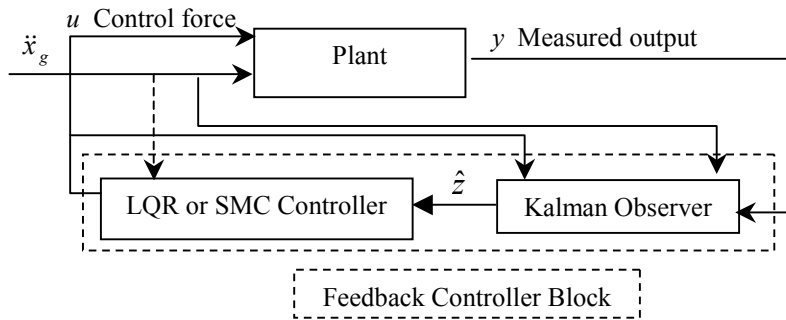
Figure 1: Control block diagram